Capillary phenomena in extremely thin zeolite channels and metal-dielectric interaction

V. N. Bogomolov
A. F. Ioffe Physical Technical Institute, Polytechnicheskaya Street 26, 194021 Street Petersburg, Russia
(Received 9 March 1995)

The experimental results on capillary phenomena in channels of atom-scale diameters comparable with the interface transition layer thickness (1–1.5 Å) are reported. A simple model for the interface metal-dielectric layer is proposed. It is based on the van der Waals bond as a weak excimer interaction of the fluctuation origin. Some aspects of interphase interaction as applied to adsorption, catalysis, energetics, and electronics are discussed.

Investigations of capillary phenomena began early in the 19th century; however, some important problems still remain unresolved. For instance, such questions as the local structure and properties of the interface layers (the Tolman length[1]), static and dynamic properties of the interphase interaction (wetting[2]), the capillary phenomena in extremely thin channels, or the transition from capillary to diffusion phenomena are not completely understood. The tension at the surface of a liquid is one of the more striking manifestations of the forces that act between atoms and molecules. The reestablishment of a direct link between capillary phenomena and the interatomic forces depends on the development of the statistical mechanics of the systems that are highly inhomogeneous on the scale of length of the range of these forces.[1]

The case when the transition layer thickness is comparable with the capillary radius r is of special interest. In the first approximation of the Gibbs thermodynamics the thickness of the transition layer is taken to be zero. In this case an effective density of the surface energy σ_s is ascribed to some interphase surface (surface of tension with curvature of radius r_s). Then the interphase pressure P, the surface energy σ_s, and the curvature radius r_s are related by the Laplace equation $2\sigma_S = Pr_s$. The real properties of the transition layers could be taken into account by the choice of some effective parameters. In this approach σ_s does not depend on r_s. However, the real interphase layers have a nonzero thickness at least on the atomic scale. Therefore bending of the layer may result in a displacement of the surface of tension as well as in the dependence of σ_s on r_s.

Figure 1 shows schematically transition layers (α and β) between two homogeneous phases A and B. The dashed line indicates the position of the surface of tension (r_s) and the solid line shows the boundaries of the homogeneous regions of these phases. For phase B the boundary coincides with an equimolar surface with radius r_e. The letters α and β denote the transition composition regions neighboring phases A and B, respectively.[1] Later it was found that there is only a single position of the surface of tension (r_s) that corresponds to the minimum of the interphase energy $\sigma_{s\min}$. This means that $\sigma_{s\min}$ is nearly independent of a small shift of r_s position relative to the phase boundaries.[3] A simple relation between σ_s and r_s was found later: $\sigma_s(r_s) \simeq \sigma(\infty)(1-2\delta/r_s)$. It is a simplified form of the expression of the well known Gibbs-Tolman-Koenig-Buff equation. The parameter $\delta = r_e - r_s$ (Fig. 1) is a formally introduced thickness of the interphase layer of one of the phases (the Tolman length). The local structure and physical parameters of this layer have not been clarified yet. This is due to experimental difficulties encountered in measurements of very thin layers. Their thickness is estimated to be 1–2 Å for inert gases[3] and about 0.2–0.6 Å for metals.[4] The value δ is quite small compared with the size of atoms.

These interphase transition layers are among the most important objects because their properties are responsible for the heterogeneous equilibrium, the rate of chemical reactions, the catalytic and geological processes, morphogenesis and exchange processes in living organisms, operation and stability of many solid-state electronic devices, and so on.

Thus the examination of the problem calls for investigation of the capillary phenomena in channels of atomic size $a \simeq 3$ Å and taking into account the interface layers $D > a + 2\delta \simeq 6$–7 Å.

Such channels are available in zeolite single crystals as their structural components.[5] The high density of channels (their total volume is up to 50% of the whole crystal volume) and the absence of dangling bonds at the internal channel surface make these crystals very suitable objects

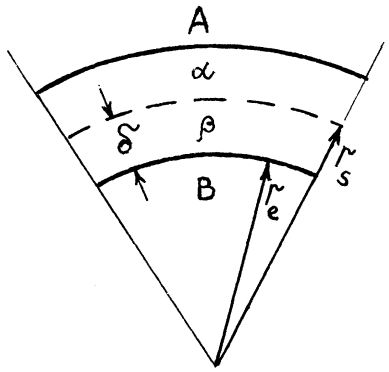

FIG. 1. Thermodynamics scheme of the interface layer.

0163-1829/95/51(23)/17040(6)/$06.00

for studying the capillary phenomena in extreme conditions. The Laplace pressure for liquid metals in these channels is about $(20-30)\times10^3$ atm. Some complications arise from the channel arrangement and their surface relief: channel crossing and spherical or cylindrical shape with both positive and negative curvature. Zeolites are aluminosilicates with a framework formed by the tetrahedral units $(Al,Si)O_4$ (Fig. 2). The charge difference between Al- and Si-based tetrahedra is compensated by the charge of alkali ions located at the channel surface. Tetrahedron dimensions are determined by the oxygen ion diameter equal to 2.7 Å. Figure 3 shows a cross section of the zeolite mordenite (M) unit cell $20.5\times18.2\times5.7$ Å^3 in size in the plane perpendicular to the axes of one-dimensional channels. The average channel diameter is about 6.6 Å (dashed circle). The aluminosilicate framework of mordenite consists of specific chains in which the five-membered rings of tetrahedra prevail (in Fig. 3 the tetrahedra vertices are linked by lines). The Hg atom of diameter 3.2 Å is shown in the center channel for scale reference. The free volume of wide channels in mordenite is 18–19 % of the total crystal volume. This value follows from both the structure consideration and the evaluation of the amount of wetting liquid (H_2O) which entirely impregnates the channels.

$(Al,Si)O_4$ tetrahedra may be put together in the cubo-octahedron form ("spheres" N_{60})-$(Al,Si)_{24}O_{36}$ (Fig. 4). Solid lines connect the centers of tetrahedra. Depending on the combination of these cubo-octahedra in the three-dimensional lattice a zeolite of A or X type is formed. The cubo-octahedra are linked to each other by four six-membered oxygen rings of free diameter 4.1 Å form zeolite X. Figure 4 demonstrates a fragment of the zeolite X unit cell. The supercage of diameter 11.7 Å possesses four windows, each 8.4 Å in diameter. Supercages form the diamond-type lattice with a lattice constant 24.6 Å. Between the adjacent supercages inside the windows (8.4 Å in diameter $=2r_2$) there are cross sections with negative curvature ($2r_3=8.2$ Å). Thus the total Laplace pressure is determined by the supercage diameter (11.7 Å) alone, because for window effective curvature $1/2r_w=1/8.4-1/8.2<0$. This means that in the window region there is an effective wetting for liquid metals. The supercage volume is about 47% of the crystal volume (28 H_2O molecules per supercage). The Hg atom in the supercage is shown in Fig. 4.

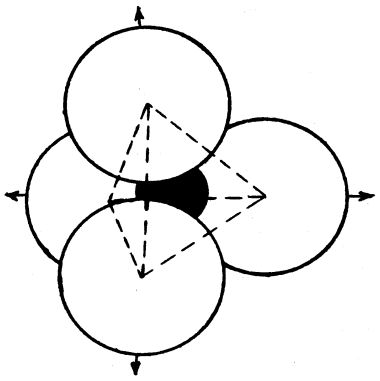

FIG. 2. Structural component of zeolites, aluminosilicate tetradhedron $(Al, Si)O_4$.

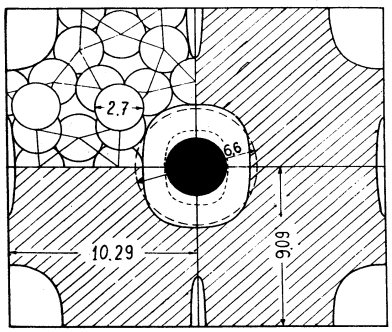

FIG. 3. Modernite unit cell in the plane perpendicular to the wide channel axis direction. Si and Al atoms are not shown. The effective diameter and border of the interphase gap are designated by the dashed lines.

The cubo-octahedra linked together by six four-membered oxygen rings give the lattice of zeolite A (Fig. 5). In this case the supercages of 11.2 Å in diameter form a cubic lattice with the lattice constant 12.4 Å and free volume 43%. The supercage windows are 4.2 Å in diameter. In Fig. 5 the Hg atom is shown in the center of the window. The Laplace pressure is also determined by the diameter of the supercage alone but not by the window diameter owing to the presence of both positive and

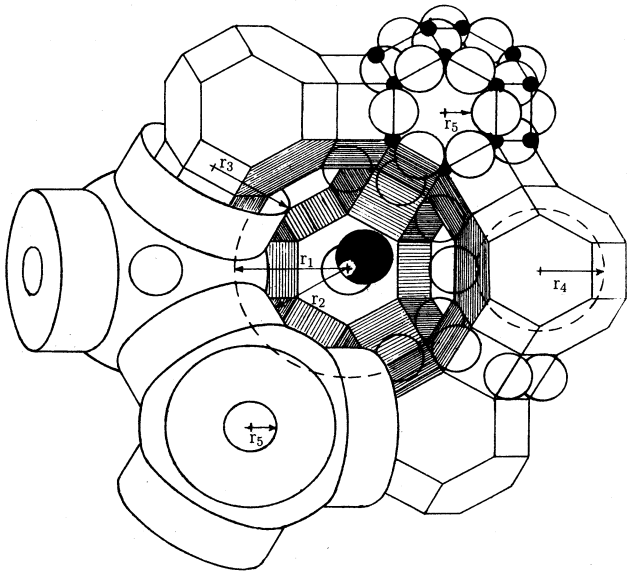

FIG. 4. Component of zeolite X structure. The cubo-octahedra $N_{60}\rightarrow(Al,Si)_{24}O_{36}$ of about 11 Å in diameter joined through the six-membered oxygen rings form the supercage of $2r_1=11.7$ Å in diameter with four windows of $2r_2=8.4$ Å in diameter. The diameter of the oxygen ring is $2r_3=8.2$ Å. N_{60} spheres have the cage of $2r_4=6.6$ Å diameter connected with the supercage through the windows with diameter $2r_5=1.8$ Å. The black circle is an Hg atom 3.2 Å in diameter.

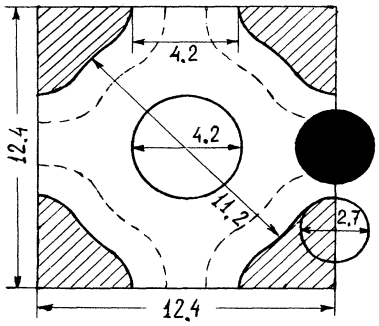

FIG. 5. Cross section of an A zeolite unit cell by the plane (0,0,2). The atoms of oxygen from zeolite framework as well as Hg atom of 3.2 Å in diameter are shown for reference. The dashed line designates the border of the interphase gap.

negative curvatures in the diaphragm region.

The structural unit N_{60} of X- and A-type zeolites has a diameter of nearly 11 Å and looks like the structural unit C_{60} of fullerenes. This similarity between zeolites and fullerenes has already been mentioned.[6] In Fig. 6 the equivalent channels for three types of zeolites with the Hg atom (labeled 2) in the narrowest place of the channel are shown schematically. The oxygen atoms are labeled as 1. It is obvious that the concept of the effective Laplace curvature at $D < a$ lose its meaning. At $D < a$ the diaphragm permeability has to be determined by statistical factors. For instance, the Laplace pressure for liquid metals in the channels of zeolite A exceeds that of zeolite X only by 10–20% whereas $D_A/D_X \simeq 1/2$. For wetting liquids zeolites were used as molecular sieves for a long time. For nonwetting liquids filtration through zeolite channels was also observed (for instance, penetration of Sn atoms into the channels from the Ga melt).[7] The penetration ability of various atoms into zeolite channels depends on the surface tension and Laplace pressure, but not on the atom diameter.

Zeolites are highly stable under heating up to 800 °C (Ref. 5) and do not reveal any lattice damage under quasihydrostatic pressure of 40×10^3 atm. Since about half of X and A zeolite crystal volume is the crystallographic cavities, the complete collapse of their lattice under high pressure is accompanied by nearly twofold volume reduction and conversion of elastic energy to heat (about 4000 kcal/kg). Experimentally we have achieved

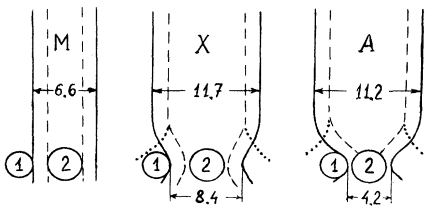

FIG. 6. Schematic representation of channels in M, X, and A zeolites. 1, oxygen atom; 2, mercury atom. The dashed lines indicate the border of the interphase gap. The dotted line indicates the Laplace radius $r^{-1} = r_1^{-1} + r_2^{-1}$ in the diaphragm region.

the complete amorphization of zeolite X at about 10^6 atm only.

In our experiments the M, X, and A zeolite channels were impregnated by liquid metals with rather low melting points (see Table I). The samples of commercial zeolites (powder consisting of 5–10-μm crystals) in the form of tablets were encapsulated in the hermetic thin-walled metallic containers together with liquid metals and then were compressed using ordinary piston chambers. Friction losses did not exceed 5–10%.

Figure 7 shows typical P-v diagrams for zeolite-metal systems. The compressibility of the chamber, zeolite, and liquid metal were measured under pressure $p < P_k$ where the liquid metal does not penetrate into zeolite channels (P_k is the critical Laplace pressure). This value of compressibility was subtracted from the compressibility for the $P > P_k$ region. The obtained P-v dependences clearly reveal two specific features. First, the liquid metal occupied about a half the free cage volume of zeolite X. The vertical dashed line indicates the total volume occupied by wetting liquid (H_2O), i.e., the total volume of crystal cavities. Assuming that the second half of the cage volume falls on the interface layer, one can find the layer thickness $h \simeq 1.2$–1.5 Å. In Figs. 3, 5, and 6 the position of this layer is marked by the dashed line.

The vast surface of the metal-zeolite contact (about 10^7 cm^2/g) leads to a large volume of the interface layer (about 25% of the total volume of the crystal).

Second, the reduction of the total volume of the system at $P > P_k$ (Fig. 7) is the result of penetration of the liquid metal into the zeolite channels. Assuming that the interface layer (interphase gap) undergoes compression its compressibility can also be estimated as $\kappa \simeq (40-50) \times 10^{-6}$ atm. These facts are in agreement with the assumption of the van der Waals (vdW) type of metal-dielectric interaction. Solid inert gases exhibit the compressibilities of the same order of magnitude. This is not surprising. For inert gase the vdW radii in solids are close to the excited-state orbitals' radii and exceed the ground-state orbitals' radii by 1.2–1.4 Å. The compressibility of the solid inert gases is determined by the response of the "gap" on the external pressure. The dependencies of the critical (Laplace) pressure $P_k(\sigma_0)$ on the surface tension of metal σ_0 for X and M zeolites are shown in Fig. 8. To analyze the experimental data it is necessary to define the values of surface energies and to make use of the equations of the capillary phenomena theory. The dielectric–liquid-metal contact with the transition layer h is shown in Fig. 9. The surface energies of liquid metals at moderate temperatures (relative to the critical values) differ from the surface tension only slightly.

The following symbols and equations are used: σ_0, the surface energy of liquid metal (300–700 ergs/cm^2); σ_t', the surface energy of solid dielectric (for zeolite it is equal to 800–900 ergs/cm^2); σ_{t0}, the interphase surface energy; σ_t, the effective surface energy of solid dielectric; σ_c, the adhesion energy; α, the contact angle;

$$\sigma_t = \sigma_{t0} - \sigma_0 \cos\alpha \ , \tag{1}$$

the Young equation;

TABLE I. Experimental data and calculated parameters for the molten metals embedded in the channels of X and M zeolites. σ is in ergs/cm^2; P_k in kbar; d,h,δ in Å, κ in 10^{-6} atm^{-1}. σ_0 is the surface tension, P_k the Laplace pressure, h the interphase gap, d the diameter of metal pillar, δ_0 the Tolman length, $\sigma_k=\sigma_0-\sigma_c$,$\sigma_c$ the adhesion energy, σ_t an effective surface energy of solid dielectric, σ_{t0} the interphase surface energy, and κ an "interface compressibility."

NaX	σ_0	P_k	h	d	δ_0	σ_k	σ_c	σ_t	σ_{t0}	κ
Bi	370	6.5	1.2	9.3	0.50	138	232	36.5	175	50
Pb	450	10	1.6	8.4	0.22	200	250	35.0	235	a
Hg	470	9.6	1.2	9.3	0.32	209	261	36.0	245	46
Cd	540	11	1.6	8.4	0.22	219	320	47.5	267	41
Sn	540	11.3	1.6	8.4	0.22	225	315	46.0	271	44
In	550	14	1.6	8.4	0.22	270	279	35.5	307	39
Ga	715	20	1.4	8.7	0.30	398	317	35.0	433	41
NaM										
Bi	370	20	1.5	3.6	0.50	135	235	37	172	38
Hg	450	29	1.7	3.2	0.32	186	263	38	225	a

[a]Technical difficulties do not allow us to increase the pressure much higher than P_k where the reliable determination of κ would be possible.

$$\sigma_{t0}=\sigma_0+\sigma_t-\sigma_c \ , \tag{2}$$

the Dupre equation;

$$P=\sigma_k(1/r_1+1/r_2) \ , \tag{3}$$

$$\sigma_k=\sigma_0-\sigma_c=\sigma_0\cos\alpha \ ,$$

the Laplace equation

$$\sigma_c\simeq 2(\sigma_0\sigma_t)^{1/2} \ , \tag{4}$$

the Girifalco-Good equation[8] (the Berthelot relation);

$$\sigma_{t0}^{1/2}=\sigma_0^{1/2}-\sigma_t^{1/2} \ , \tag{5}$$

this follows from (2) and (4);

$$\sigma(r_s)=\sigma(\infty)B(\delta/r_s)\simeq\sigma(\infty)r_s^2/(r_s+\delta)^2 \simeq\sigma(\infty)(1-2\delta/r_s) \tag{6}$$

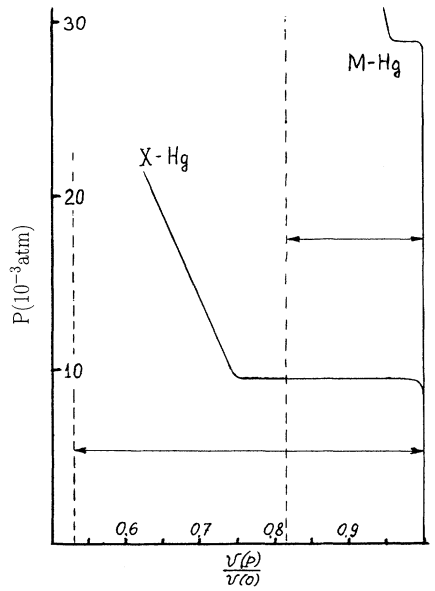

FIG. 7. The relative volume $v(P)/v(0)$ vs P for zeolite X-mercury and zeolite M-mercury systems. The dashed lines indicate the total free volume of channels in X and M zeolites.

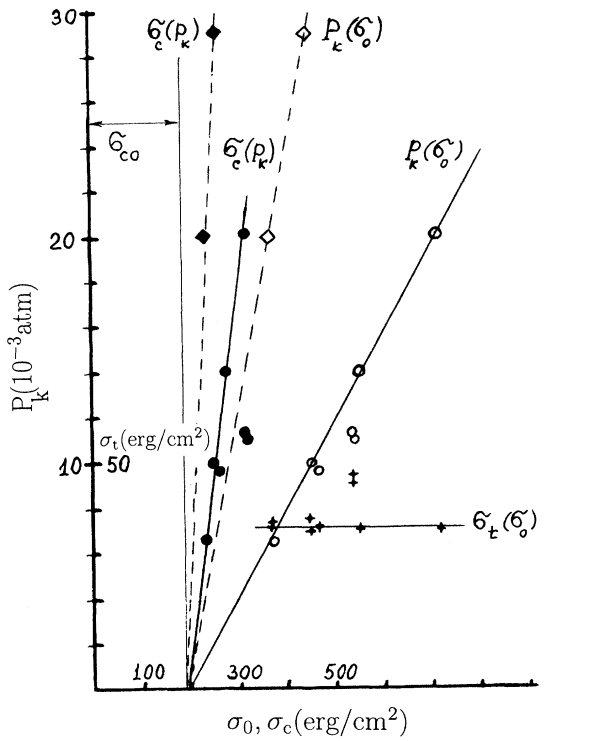

FIG. 8. Dependencies of the critical pressure P_k on the surface tension for metal σ_0 (see Table I) for X zeolite (open circles) and M zeolite (open squares). Dependencies of the adhesion energy σ_c on P_k for X zeolite (dark circles) and M zeolite (dark squares). The dependence of an effective surface energy of solid (zeolite) σ_t on σ_0 (crosses).

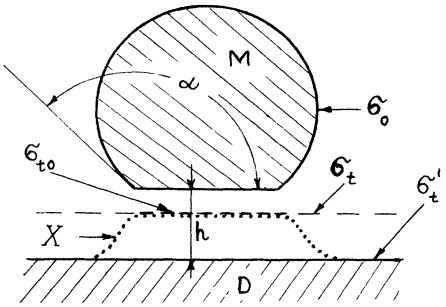

FIG. 9. Schematic representation of contact metal dielectric (zeolite). X, the average probability of the surface excited state occupation.

the Gibbs-Tolman-Koenig-Buff equation;[3]

$$\sigma(r)=\sigma(\infty)-\delta P_k \ , \tag{7}$$

from (3) and (6); δP_k, the "elastic" energy (the part of the surface energy),

$$d\sigma/dP=-\delta=-(r_e-r_s) \ , \tag{8}$$

the Tolman length (Fig. 1);

$$d\sigma/dT=-\delta_T \ , \tag{9}$$

the entropy of surface $(-0.05--0.5)$ ergs/cm^{2}K for metals) and

$$d\sigma/dP=-(\gamma/C_V)d\sigma/dT \ , \tag{10}$$

the sequence of the relation $\sigma \propto a^{-n4}$, where γ is the Grüneisen constant, C_V the volumetric specific heat, a the interatomic distance, $d\sigma/dP \simeq \frac{1}{3}n\kappa\sigma$, and $d\sigma/dP=-\delta_0 \simeq 2\sigma_0\kappa$ the Tolman length for metals; $n \simeq 6$, $\delta_0=-(0.2-0.6)$ Å,

$$\sigma_c=\sigma_{c0}+\delta_c P/2 \tag{11}$$

[see (7)] is the adhesion energy for a cylindrical capillary, σ_{c0} the adhesion energy for the case of the absence of interphase pressure, $\delta_c=2d\sigma_c/dP$, and

$$d\sigma_{t0}/dP=\delta_{t0}=\delta_0+\delta_t-\delta_c \tag{12}$$

the interphase Tolman length.

To determine the parameters of metal-dielectric contact in the atomic-scale channels it is necessary to take into account the channel size and the interphase interacting using Eqs. (1)–(12). If pressure is measured in kbar, length in Å, and energy in ergs/cm^2 we can represent

$$P_k=0.4(\sigma_0-\sigma_c)/d(1-2\delta_k/d)^2 \ ,$$

$$\delta_k=\delta_0(\sigma_0-\sigma_c)/\sigma_0$$

[see (10)],

$$\sigma_c=\sigma_0-2.5P_k d(1-5\delta_0 P_k/\sigma_0)^2$$

$$=\sigma_{c0}+5P_k\delta_c \ ,$$

$$\sigma_t=\sigma_c^2/4\sigma_0$$

[see (4)].

The elastic interphase energy $\delta_c P_k/2$ depends on δ_c and gives the main contribution to δ_{t0} [see Eqs. (11) and (12)]. The diameter d of the metal pillar in the channel is less than the channel diameter D by $2h$ (see Table I). The dependencies $P_k(\sigma_0)$ and $\sigma_c(P_k)$ for zeolite X (Fig. 8) lead to the following values: $\sigma_{c0} \simeq 190$; $\sigma_t \simeq 35-36$; $\delta_c \simeq +1.3$ Å [δ_c is determined from the slope of the σ_c-P_k curves (Fig. 8)]. The rough calculated value δ_c is about $2\sigma_c\kappa \simeq 1.5$ Å according to (10).

In channels of mordenite only one atom of Hg or Bi can be located on a cross section of the channel. The experimental results are in a good agreement with this statement. So, the amounts of Hg and Bi introduced into mordenite (3.7% and 6% of the crystal volume) are nearly proportional to the ratio of their atom cross sections $(3.2/3.6)^2=0.79$ and correspond to single atomic chains. In this case the interphase pressure should be much lower than half the Laplace pressure because in a single atomic chain the transverse pressure can be only due to thermal vibrations and chain bending. This is revealed in a reduction of the adhesion energy due to a decrease of the contribution related to the interphase pressure $\delta_c P_k/2$. The length δ_c for mordenite (0.5 Å) is less than that for the X zeolite (1.5 Å). In other respects the capillary phenomena in the mordenite channels retain their character: $P_k \propto 1/D$; $\sigma_{c0} \simeq 190$; $h \simeq 1.5$ Å.

Thus the capillary phenomena in the atomic-scale channels comparable with the interface layer thickness can be adequately described in terms of the modern theory of capillarity.

The surface tension depends on the electronic structure of atomic shells. Figure 10 shows the dependence of surface tension of (3-4-5)d^m metals on number m for d electrons. One can see that an increase in m up to $m=5$ is accompanied by an increase of σ ($\sigma \simeq m \times 1000$ ergs/cm^2). The surface tension is proportional to the number of unpaired electrons. The following increase of m leads to a decrease of σ due to electron pairing. Such dependence of the surface tension on electric structure of atoms is true for s and p electrons also. For monophase metallic systems the surface tension σ increase with decreasing drop diameter as shown in (6) and (8). It is easy to show that in the limit $2r \to a$ the increase of σ manifests itself an an effect of the Goldschmidt contraction when the atomic diameter decreases by about 20%. This value is consistent with the difference between the diameter of an atom in the metal bulk (in the limit $r \to \infty$) and

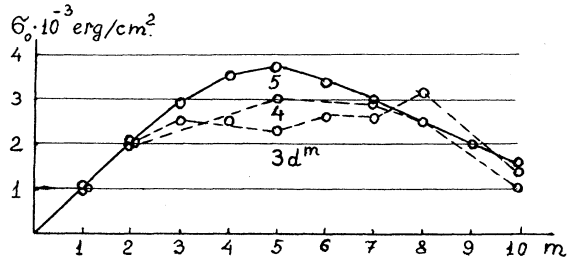

FIG. 10. The dependence of the surface tension on m for (3-4-5) d^m elements.

a free atom ($r=a/2$).[9]

Besides the two peculiarities of the capillary phenomena in channels of the atom-scale diameters (the existence of gap h and its compressibility κ) the analysis of the experimental data (Fig. 8) reveals a third unusual feature. The effective "interphase" surface energy of solid dielectric $\sigma_t \simeq 36$ ergs/cm^2 is much less than the intrinsic one of solid dielectric $\sigma_t' = 800$ ergs/cm^2 (Fig. 9). The latter was measured calorimetrically and calculated using the Berthelot relation to evaluate the adhesion heat of H_2O. This relation was used by Pauling as the basis of the electronegativity scale. No doubt the difference is caused by the presence of the vdW interaction and the appearance of corresponding equilibrium distances of about h, similarly to the case of condensed inert gases. If one takes into account a similarity between the vdW radii for the latter and the radii of the excited state orbital (excimers) the following simple model of the metal-dielectric interface may be proposed. As a metal atom approaches a dielectric surface, the surface atoms of the dielectric are excited by the Coulomb perturbation with transition of electrons to the excited-state orbitals. This process is determined by an average occupation factor X for the excited-state orbitals (the dotted line in Fig. 9). For the atoms of the dielectric $X<1$.

Thus, the surface of the dielectric "swells" by a layer of thickness $\propto h$ on contact with metal. The electrons of the metal ($X_0=1$) interact with the virtually excited electrons of the dielectric surface and in this case the adhesion energy is $\sigma_c \propto e^2 X/r_{\rm av}$, where e is the electron charge and $r_{\rm av}$ is the average distance between atoms.[4] It is easy to see that this model satisfies the Berthelot relation $\sigma_c \propto (e^2e^2X^2)^{1/2} \propto (\sigma_0\sigma_t)^{1/2}$ at $\sigma_t \propto e^2X^2$ and $\sigma_0 \propto e^2$ because $X_0=1$ for metal. The interface surface energy σ_{t0} is determined by the difference in probabilities of occupation of the electron states $X_{t0}=X_0-X_t=1-X_t$ on the interphase surface [Eq. (5) and Figs. 1 and 9]. As mentioned above, the channel surface in zeolites is of "molecular" origin since it does not have dangling bonds. Over the channel surface there will be excited-state orbitals only. In this case the concept of the vdW bond as the weak excimerlike interaction of the fluctuation origin can be used. The information about the interface metal-dielectric layers is useful not only for the capillary phenomena physics but for ultradisperse heterogeneous systems also. Using Eqs. (10) and (12) one can estimate the interphase Tolman length: $\delta_{t0}=d\sigma_{t0}/dP \simeq 2\sigma_0\kappa_0 + 2\sigma_t\kappa_h - \delta_c$.

Since the first two items are of the same order of magnitude (10) and less than δ_c, then $d\sigma_{t0}/dP<0$ and the interphase surface energy decreases when the interphase pressure (or the curvature of surfaces) increases (pressure-assisted reactions, dissolution, and so on). In heterogeneous catalysis on the metal surfaces the adsorbed molecules of reagents A and B can interact with each other being in the excited states whose probability is X_m. The energy of interaction of the reagents on the metal surface is proportional to $X_mX_{mB} > X_AX_B$, where the latter determines the energy of interaction without the metal surface assistance.

Nanostructures based on the heterogeneous ultradisperse systems are finding ever increasing application. Therefore properties of thin interphase layers between different materials are very important for the design and properties of novel devices or novel materials (for instance, one-dimensional superlattices[10] or cluster crystals[11]). The appearance of excited states in the transition layer can be responsible for luminescence of ultradisperse materials.

Zeolites that contain liquid metals in their channels are heterogeneous systems with a great amount of surface energy. From the data shown in Fig. 7 one can estimate the mechanical energy capacity to be 200 kJ/liter. Such systems can be used for constructing accumulators of mechanical or electrical (supercapacitor) energy. Their power consumption is approaching that of electrochemical batteries.[12] The systems also can be used for refrigerators and electrical engines with specific power which is 10–100 times more than that of electrical motors.[12] The study of capillary effects in systems with extremely high dispersion is evidently of both scientific and practical interest for problems of chemical technology, electronics, energetics, and environmental engineering.

ACKNOWLEDGMENT

The research described in this publication was made possible in part by Grant No. R1X000 from the International Science Foundation.

[1] J. S. Rowlinson and B. Widom, *Molecular Theory of Capillarity* (Oxford University, New York, 1982).
[2] P. G. De Gennes, Rev. Mod. Phys. **57**, 827 (1985).
[3] S. Ono and S. Kondo, *Molecular Theory of Surface Tension in Liquids* (Springer-Verlag, Berlin, 1960).
[4] V. N. Bogomolov, Zh. Tekh. Fiz. **62**, 152 (1992) [Sov. Phys. Tech. Phys. **37**, 79 (1992)]; Phys. Solid State **35**, 469 (1993).
[5] D. W. Breck, *Zeolite Molecular Sieves* (Wiley, New York, 1974).
[6] M. O'Keeffe, Nature **352**, 674 (1991).
[7] V. N. Bogomolov, A. I. Zadorozhnii, and N. A. Klushin, Fiz. Tverd. Tela Leningrad **17**, 2452 (1975) [Sov. Phys. Solid State **17**, 1627 (1975)].
[8] L. A. Girifalco and P. Good, J. Phys. Chem. **61**, 904 (1957); **64**, 561 (1960).
[9] J. T. Waber and D. T. Cromer, J. Chem. Phys. **42**, 4116 (1965).
[10] L. L. Chang and L. Esaki, Phys. Today **45** (10), 36 (1992).
[11] V. N. Bogomolov, Usp. Fiz. Nauk **124**, 171 (1976) [Sov. Phys. Usp. **21**, 77 (1978)].
[12] V. N. Bogomolov, Tech. Phys. **38**, 224 (1993).